Developmental Cell
Article

Hoxb5b Acts Downstream of Retinoic Acid Signaling in the Forelimb Field to Restrict Heart Field Potential in Zebrafish

Joshua S. Waxman,[1] Brian R. Keegan,[1] Richard W. Roberts,[2] Kenneth D. Poss,[2] and Deborah Yelon[1,*]
[1]Developmental Genetics Program and Department of Cell Biology, Kimmel Center for Biology and Medicine at the Skirball Institute of Biomolecular Medicine, New York University School of Medicine, New York, NY 10016, USA
[2]Department of Cell Biology, Duke University Medical Center, Durham, NC 27710, USA
*Correspondence: yelon@saturn.med.nyu.edu
DOI 10.1016/j.devcel.2008.09.009

SUMMARY

How adjacent organ fields communicate during development is not understood. Here, we identify a mechanism in which signaling within the forelimb field restricts the potential of the neighboring heart field. In zebrafish embryos deficient in retinoic acid (RA) signaling, the pectoral fins (forelimbs) are lost while both chambers of the heart are enlarged. We provide evidence that both of these phenotypes are due to RA signaling acting directly within the forelimb field. *hoxb5b*, an RA-responsive gene expressed within the forelimb field, is required to restrict the number of atrial cells arising from the adjacent heart field, although its function is dispensable for forelimb formation. Together, these data indicate nonautonomous influences downstream of RA signaling that act to limit individual chamber size. Therefore, our results offer new perspectives on the mechanisms regulating organ size and the possible causes of congenital syndromes affecting both the heart and forelimb.

INTRODUCTION

The early vertebrate embryo can be thought of as a collage of organ fields, partially overlapping zones of developmental potential that envelop their respective pools of organ progenitor cells (Fishman and Chien, 1997; Huxley and deBeer, 1934; Jacobson and Sater, 1988). Over time, refinement of developmental potential narrows each field into the precise dimensions of the organ primordium. The gradual restriction of organ fields is therefore one important mechanism for controlling organ size. The proximity and overlap of developing fields suggests that communication between adjacent territories could contribute to organ field restriction, but little is known about whether neighboring fields coordinate their development.

The embryonic heart field is an interesting example of a zone of developmental potential that becomes restricted over time. Several studies have demonstrated that cardiac developmental potential extends beyond the boundaries of the region of the lateral plate mesoderm (LPM) that normally becomes myocardium. For example, Notch signaling plays a role in repressing cardiac specification in a lateral portion of the *Xenopus* LPM that normally forms mesocardium and pericardium (Raffin et al., 2000; Rones et al., 2000). In zebrafish, components of the vascular and hematopoietic specification pathways, particularly the transcription factors Scl and Etsrp, inhibit cardiac specification in rostral LPM (Schoenebeck et al., 2007). There appear to be multiple pathways that restrict the plasticity of the heart field, and it is likely that additional inhibitory mechanisms remain to be characterized.

Our recent studies have revealed that the retinoic acid (RA) signaling pathway plays a potent role in limiting cardiac specification. Zebrafish embryos lacking RA signaling exhibit a surplus of cardiomyocytes, a consequence of an excess of cardiac progenitor cells (Keegan et al., 2005). More recently, it has also been demonstrated that mouse embryos lacking the RA synthesis enzyme Raldh2 display an expansion of the second heart field (SHF), a territory that contributes to both the inflow and outflow poles of the amniote heart (Ryckebusch et al., 2008; Sirbu et al., 2008). It is not yet apparent how this newly identified early role of RA in restricting the SHF fits together with a previously hypothesized role of RA signaling during cardiac fate assignment in amniotes. Specifically, it has been proposed that RA signaling promotes atrial cell identity within the heart field, thereby defining the relative proportions of atrial and ventricular cells (Hochgreb et al., 2003; Xavier-Neto et al., 1999, 2001). It remains unknown whether the proposed roles of RA in promoting atrial identity and in restricting the SHF are distinct or overlapping. Moreover, it is unclear where and how RA acts to restrict cardiac specification.

The impact of RA signaling on the forelimb field may provide clues to the mechanisms by which RA restricts the size of the heart field. In both zebrafish and mouse embryos that lack RA signaling, there is a converse relationship between heart and forelimb formation: forelimbs are lost, while the number of cardiac cells is increased (Keegan et al., 2005; Niederreither et al., 1999; Ryckebusch et al., 2008; Sirbu et al., 2008). Previous studies in both organisms have indicated that RA signaling induces formation of the forelimb field by promoting *tbx5* expression (Begemann et al., 2001; Gibert et al., 2006; Mercader et al., 2006; Mic et al., 2004). However, it is not known whether this reflects a direct requirement for RA signaling within forelimb progenitor cells. It is tempting to speculate about a connection between the mechanisms that result in forelimb deficiency and cardiac surplus. One possibility is that reduction of RA signaling converts forelimb progenitors into heart progenitors, or perhaps effects of

RA on one field have indirect consequences for the other. Alternatively, RA may impact the development of each field independently. The possibility of coordinate regulation of the heart and forelimb fields is likely to be relevant to the causes of human congenital defects that affect both tissues, including inherited heart-hand syndromes (Wilson, 1998).

In this study, we sought to address where and how RA signaling limits the number of cardiac progenitor cells in zebrafish. We find that RA signaling restricts the numbers of both atrial and ventricular cardiomyocytes, through independent effects on each lineage. Loss of RA signaling leads to a posterior extension of both atrial and ventricular progenitor cells into territory normally occupied by forelimb progenitor cells. We show that RA signaling is required cell-autonomously for forelimb formation. However, posterior extension of the heart field in embryos lacking RA signaling does not seem to reflect a transformation of forelimb progenitor cells into cardiac progenitor cells. Additionally, we demonstrate that expression of *hoxb5b* in the forelimb field is RA responsive. Strikingly, *hoxb5b* plays an essential and nonautonomous role in restricting the number of atrial cardiomyocytes that emerge from the heart field. Together, our data indicate that RA signaling, through its direct effect on forelimb field formation, acts indirectly to limit the specification of cardiac progenitors within the heart field; thus, interactions between adjacent organ fields play an important role in the refinement of developmental potential. These findings provide a new perspective on the regulation of organ size and may yield insight into the etiology of human heart-hand syndromes.

RESULTS

RA Signaling Restricts the Numbers of Both Atrial and Ventricular Cells

We have recently demonstrated that RA signaling plays an important role in restricting the production of cardiac progenitor cells in the zebrafish embryo (Keegan et al., 2005). However, this study did not elucidate the mechanisms downstream of RA signaling that are responsible for heart field restriction. As a first step toward this goal, we sought to determine whether RA signaling has comparable effects on both the atrial and ventricular lineages. Therefore, we examined cardiac chamber formation in embryos that were treated with either the retinaldehyde dehydrogenase inhibitor DEAB (Russo et al., 1988) or the RA receptor antagonist BMS189453 (BMS) (Schulze et al., 2001) beginning at 40% epiboly, just before the onset of gastrulation.

At 48 hr postfertilization (hpf), atrial and ventricular chambers were distinct and easily identifiable in wild-type embryos (Figure 1A), as well as in embryos treated with DEAB or BMS (Figures 1B and 1C). However, the hearts of DEAB-treated or BMS-treated embryos were highly dysmorphic and typically appeared enlarged. We counted the cardiomyocytes in each chamber to determine if aberrant morphology reflected a change in cell number. Both DEAB and BMS treatments led to a significantly increased number of atrial and ventricular cells (Figures 1D and 1E; see Table S1 available online). Increases in atrial and ventricular populations were also apparent prior to heart tube formation, as indicated by the expression patterns of the earliest known chamber-specific genes, *atrial myosin heavy chain* (*amhc*) (Berdougo et al., 2003) and *ventricular myosin heavy chain* (*vmhc*) (Yelon et al., 1999) (Figures 1F–1K; Table S2). The phenotypes resulting from treatments with BMS or DEAB resembled those resulting from treatment with Ro41-5253 (RO, an RARα-specific antagonist) or from loss of *raldh2* gene function (Figures S1 and S2; Tables S1 and S2; J.S.W. and D.Y., unpublished data). Together, these data show that RA signaling is required to restrict the numbers of both atrial and ventricular cells in zebrafish.

Reduction of RA Signaling Increases the Numbers of Atrial and Ventricular Cells through Independent Mechanisms

To refine our understanding of when RA signaling is required to limit the numbers of atrial and ventricular cells, we next compared the effects of initiating BMS treatment at different developmental stages. We found a progressive decrease in sensitivity to BMS over time. Both atrial and ventricular populations are significantly enhanced when BMS treatment occurs during gastrulation (Figures 1D and 1E; Table S1), similar to our previous findings (Keegan et al., 2005). However, by the 6–8 somite stage, only atrial cells, not ventricular cells, are affected by BMS treatment (Figures 1D and 1E; Table S1). This temporal difference in sensitivity to BMS treatment is compatible with the notion that ventricular differentiation normally precedes atrial differentiation (Berdougo et al., 2003) and suggests that RA signaling might limit atrial and ventricular cell number through different mechanisms.

To determine whether RA signaling has a similar impact on both atrial and ventricular progenitor specification, we next examined cardiomyocyte progenitor fate maps from wild-type and BMS-treated embryos (Figure S3; Table S3). Comparison of the wild-type and BMS-treated fate maps demonstrated that BMS treatment does not significantly disrupt the relative spatial organization of atrial progenitors (APs) and ventricular progenitors (VPs) (Figures 1L and 1M; Figure S3; Table S3). Importantly, we did not find VPs in the territory where normally only APs are found, or vice versa (Figures 1L and 1M; Figure S3), suggesting that neither increase in cell number occurs at the expense of the other lineage.

To determine whether the increases in ventricular and atrial cell number in BMS-treated embryos are due to increased numbers of VPs and APs, we compared the frequency of encountering each type of progenitor within their respective territories in the wild-type and BMS-treated fate maps. We encountered VPs almost twice as often within the ventricular territory of BMS-treated embryos as we did within the ventricular territory of wild-type embryos ($p < 0.005$; Figures 1L–1N; Figure S3; Table S3). In contrast, the frequency of encountering APs within the atrial territory did not change in the BMS-treated fate map (Figures 1L–1N; Table S3). These data indicate an increase in the number of VPs in the lateral margin of BMS-treated embryos at 40% epiboly, while the number of APs appears unaffected by BMS treatment at this stage.

Although BMS treatment did not affect the density of APs at 40% epiboly, we did observe a striking effect of BMS on the number of labeled progeny produced per AP. Our fate map data indicated that APs in BMS-treated embryos generated an increased number of atrial cardiomyocytes compared to wild-type APs ($p < 0.05$; Figure 1O; Table S3). In contrast, we did not observe an increased number of progeny from VPs in BMS-treated embryos compared to the number of progeny

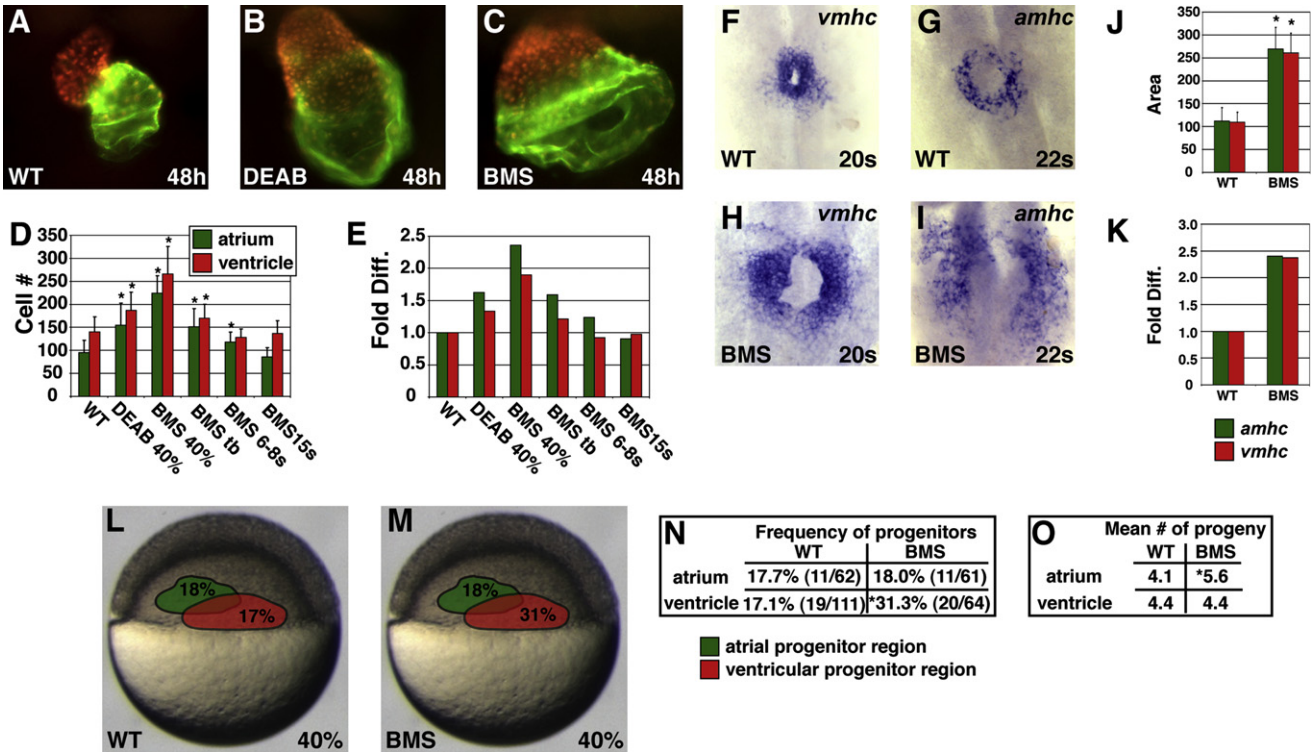

Figure 1. Reduction of RA Signaling Causes an Increase in the Number of Atrial and Ventricular Cells

(A–C) Frontal views of hearts at 48 hpf expressing the transgene *Tg(cmlc2:DsRed2-nuc)* (red). Atria are labeled with the anti-Amhc antibody S46 (green). (B and C) Treatment with 1 μM DEAB or 10 μM BMS causes cardiac chamber enlargement.

(D) Mean and standard deviation (SD) of numbers of atrial and ventricular cardiomyocytes. Stages indicate when DEAB or BMS treatment was initiated. Asterisks indicate statistically significant differences relative to wild-type ($p < 0.005$).

(E) Fold difference in mean cell numbers relative to wild-type (WT) controls.

(F–I) Reduction of RA signaling causes increased expression of *amhc* and *vmhc*. Dorsal views, anterior to the top at the 20 or 22 somite stage.

(J) Mean and SD of areas of expression of *amhc* and *vmhc* in WT and BMS-treated embryos. Asterisks indicate statistically significant differences relative to WT ($p < 0.005$).

(K) Fold difference in mean areas of gene expression relative to WT controls.

(L and M) Schematic of 40% epiboly fate maps from WT and BMS-treated embryos indicating that the relative position of regions containing APs (green) and VPs (red) is unchanged when RA signaling is reduced. Percentages indicate the frequency of encountering APs or VPs in each region.

(N) Reduction of RA signaling increased the frequency of encountering VPs, but not APs, at 40% epiboly. The asterisk indicates statistically significant difference relative to WT ($p < 0.005$).

(O) Reduction of RA signaling increased the mean number of labeled progeny produced by APs but not VPs. The asterisk indicates statistically significant difference relative to WT ($p < 0.05$).

from wild-type VPs (Figure 1O; Table S3). Therefore, our fate map data suggest that RA signaling restricts the number of atrial cells at a later stage than when it restricts the number of ventricular cells. These data are compatible with the temporal differences in atrial and ventricular sensitivity to BMS (Figures 1D and 1E), suggesting different timeframes for independent processes of ventricular and atrial specification.

RA-Responsive Genes Are Expressed in the Forelimb Field

As a next step toward understanding the mechanism through which RA signaling restricts cardiac chamber size, we wanted to identify RA-responsive genes that are expressed within the LPM during the time interval when RA signaling is required to limit cardiomyocyte production. Although there were some known targets of RA signaling, their relevance to cardiomyocyte production was unclear. Using microarrays followed by validation via in situ hybridization, we identified 12 RA-responsive genes expressed within the LPM; two examples that were positively regulated by RA signaling were *hoxb5b* and *retinol short-chain dehydrogenase/reductase* (*retSDR1/dhrs3*; referred to here as *retd*) (Figure 2; Figure S4).

Our identification of RA-responsive genes within the LPM suggested locations of RA signaling that might be related to the role of RA in restricting cardiac cell number. However, none of these genes appeared to be expressed within the heart field; instead, they appeared to be in a more posterior portion of the LPM. For example, at the 6–8 somite stages, when robust expression of *gata4* and *nkx2.5* is first evident in the heart field (Schoenebeck et al., 2007), *retd* is found in an adjacent posterior portion of the LPM (Figures S5D–S5I), and *hoxb5b* is found at an even further posterior position (Figures S5J–S5L). This observation was confirmed by measuring the distances between the posterior and anterior limits of gene expression, relative to the tip of

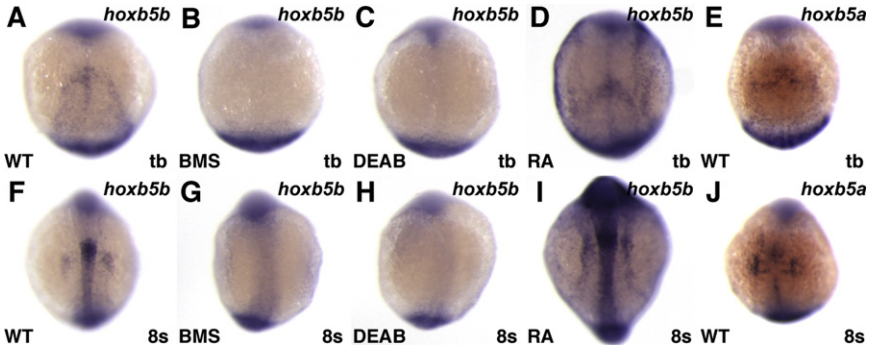

Figure 2. RA Signaling Positively Regulates *hoxb5b* Expression in the LPM

Expression of *hoxb5b* at the tailbud (tb) or 8 somite stages, dorsal views, anterior to the top.

(A–D and F–I) Reduction of RA signaling inhibits *hoxb5b* expression, and treatment with RA induces ectopic *hoxb5b* expression.

(E and J) Expression of the *hoxb5b* paralog *hoxb5a*. Identification of *hoxb5b* as a RA-responsive gene is not surprising, since the chick and mouse *Hoxb5* orthologs and the zebrafish paralog *hoxb5a* have already been implicated as direct targets of RA signaling (Bruce et al., 2001; Grandel et al., 2002; Oosterveen et al., 2003; Sharpe et al., 1998).

the notochord at the 8 somite stage (Figures 3A–3E). The posterior limits of *gata4* and *nkx2.5* expression were on average at 28 and 27 notochord cell diameters (ncds), respectively (Figures 3A and 3B; Table S4), while the anterior limits of *retd* and *hoxb5b* expression were on average at 36 and 63 ncds, respectively (Figures 3C and 3D; Table S4). The relatively posterior expression of RA-responsive genes correlates with the even more posterior location of *raldh2* expression. At these stages, *raldh2* is expressed at high levels in the somites, the most anterior of which is located on average at 72 ncds (Figure 3E; Figures S5A and S5B). The distance between *raldh2* and *gata4* expression in zebrafish contrasts with data from mouse and chick embryos where *raldh2* expression is reported to be adjacent to *gata4* at comparable stages (Hochgreb et al., 2003). Although *raldh2* begins to be expressed more anteriorly in the ectoderm in zebrafish at the 8 somite stage (Figures S5C and S5D; Grandel et al., 2002), this expression begins at the end of the time period during which RA signaling is required to limit cardiac cell number (Figures 1D and 1E). Thus, the locations of RA-responsive genes and RA synthesis suggest that RA signaling is occurring in a portion of the LPM posterior to the heart field.

We next wanted to understand how the expression patterns of RA-responsive genes related to the various progenitor populations present within the LPM. Therefore, we constructed a fate map of the relevant portion of the LPM at the 8 somite stage in wild-type embryos (Figure S6), a posterior extension of our prior fate map of the most anterior portion of the LPM (Schoenebeck et al., 2007). Our results indicated that the LPM territories containing AP and VP cells extend posteriorly to approximately 50 and 40 ncds, respectively (Figure 3F). Thus, the locations of cardiac progenitors (CPs) correlate relatively well with the expression patterns of *gata4* and *nkx2.5*, although there may be a posterior population of CPs that does not express these genes at this stage. By comparison, pectoral fin (forelimb) progenitors (FPs) were found in a territory beginning at approximately 40 ncds and extending to 60–70 ncds, corresponding to the locations of *retd* and *hoxb5b* expression. Together, our fate map data indicate that RA-responsive genes in the LPM are expressed primarily posterior to the heart field and within the forelimb field.

Loss of RA Signaling Leads to a Posterior Extension of the Heart Field

Having determined the relative positions of CPs and FPs within the wild-type LPM, we wanted to examine how loss of RA signaling and the consequential loss of FPs affects the distribution of CPs. First, we examined LPM gene expression patterns in embryos deficient in RA signaling. We found a significant lengthening of *gata4* expression in the LPM of BMS-treated, DEAB-treated, and RO-treated embryos (Figures 4A–4D; Table S5). In all cases, the change in *gata4* expression is considerably more prominent posterior to the notochord tip than it is anterior to the notochord tip. We also found similar posterior extensions of *nkx2.5* expression in treated embryos (J.S.W. and D.Y., unpublished data). Together, these results suggest that RA signaling restricts the posterior extent of cardiac gene expression within the LPM.

We were intrigued by this posterior extension of cardiac gene expression, as it suggested an enlargement of the heart field into territory that would normally contain the forelimb field. Consistent with this, we detected an altered distribution of *tbx5* expression in RA signaling-deficient embryos (Figures 4E–4H). *tbx5* is expressed in both the heart and forelimb (Ahn et al., 2002; Begemann and Ingham, 2000; Garrity et al., 2002). By the 12–14 somite stage, two slightly separated fields of *tbx5* expression appear to approximate the locations of the CPs and FPs (Figure 4E; Ahn et al., 2002). In embryos deficient in RA signaling, the separation between populations is less evident, suggesting an enlargement of the anterior population and a reduction or loss of the posterior population (Figures 4F–4H). These results confirm and extend the previous observation of a loss of *tbx5* expression in the forelimb field of *raldh2* mutant embryos at the 12 somite stage (Begemann et al., 2001). To examine whether the posterior extension of cardiac markers corresponds to a posterior extension of CPs, we constructed LPM fate maps in RA signaling-deficient embryos. Consistent with our gene expression analysis, the fate map data indicated CPs residing in posterior LPM territories that are normally occupied by FPs (Figures 3G–3I). Therefore, our data indicate that RA signaling restricts posterior extension of the heart field within the LPM.

Loss of RA Signaling Does Not Result in a Fate Transformation between Cardiac and Forelimb Progenitors

The posterior expansion of CPs into a region normally occupied by FPs suggested that a loss of RA signaling may transform FPs into CPs. One possible scenario, suggested by the expression patterns of RA-responsive genes, is that cells in the forelimb field may normally need to receive RA signaling in order to become

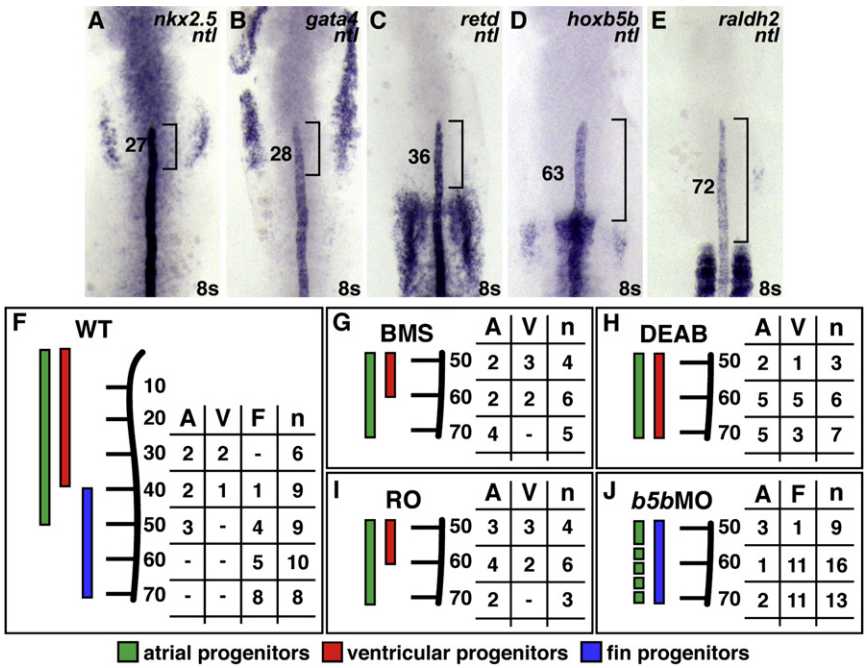

Figure 3. RA-Responsive Genes Are Expressed in the Forelimb Field

(A–E) Expression of *nkx2.5*, *gata4*, *retd*, *hoxb5b*, and *raldh2* relative to *ntl*, which marks the notochord; dorsal views of flatmounted embryos, anterior to the top, at the 8 somite stage. Brackets and numbers indicate the mean distance of the limit of gene expression relative to the tip of the notochord, measured in notochord cell diameters (ncds). (A and B) The posterior portions of *nkx2.5* and *gata4* expression overlap with the notochord. (C) *retd* expression is found posterior to *nkx2.5* and *gata4* expression. (D and E) *hoxb5b* is expressed closer to *raldh2* expression in the somites, a major source of RA in the embryo.

(F) Schematic of the WT LPM fate map at the 8 somite stage, indicating locations of atrial (green, A), ventricular (red, V), and fin (blue, F) progenitors relative to the anterior-posterior axis of the notochord, measured in ncds. Numbers in the table represent the number of labeling experiments in which each progenitor type was detected at a certain ncd position; n indicates the total number of experiments at each position. Experiments were performed on both the left and right sides of the embryo; no asymmetries were observed.

(G–I) When RA signaling is reduced, FPs are absent and CPs frequently occupy FP territory.

(J) In *hoxb5b* morphants, FPs are present and CPs rarely occupy FP territory.

FPs rather than CPs. We performed mosaic analysis to determine whether RA signaling-deficient cells would preferentially contribute to the heart rather than to the forelimb. We used two different strategies to deplete RA signal transduction in a cell-autonomous fashion: transgenic activation of a dominant-negative RA receptor or BMS treatment (Figure S7). After transplanting cells from *Tg(hsp70:dnRARα)* or BMS-treated donor embryos into wild-type host embryos, we assessed contributions of donor cells to the heart and forelimb (Figures 5A–5F). With either method of autonomously antagonizing RA signaling, we found a significant decrease in the frequency with which donor cells contribute to the fin mesenchyme (Figures 5G and 5H). Despite this indication of a cell-autonomous requirement for RA signaling during fin formation, we did not find a corresponding increase in the frequency of donor cells becoming cardiomyocytes, as would be expected if FPs were transformed into CPs (Figures 5G and 5H). Therefore, our data suggest that RA signal transduction is required cell-autonomously to promote FP formation and is most likely acting indirectly to restrict cardiac cell number.

Hoxb5b Acts Nonautonomously to Restrict Atrial Cell Number

Having established where RA signaling is acting, we next wanted to determine if any of the RA-responsive genes expressed in the forelimb field are required to limit cardiac cell number. Although anti-*retd* morpholinos (MOs) do not appear to affect fin formation or restrict cardiac cell number (J.S.W. and D.Y., unpublished data), anti-*hoxb5b* MOs do seem to disrupt heart formation. To examine the function of *hoxb5b*, we used MOs designed to block proper splicing of *hoxb5b* transcripts (Figure 6A). Despite the high similarity in target sequences, anti-*hoxb5b* and anti-*hoxb5a* MOs specifically abrogated splicing of their respective transcripts (Figures 6A and 6F). *hoxb5b* morphants (anti-*hoxb5b* MO-injected embryos) exhibit enlarged hearts and pericardial edema (Figure 6G), reminiscent of embryos with defective RA signaling. However, *hoxb5b* morphants have overtly normal fins (Figure 6H), unlike embryos lacking RA signaling. Although *hoxb5a* MOs effectively block splicing and reduce levels of wild-type *hoxb5a* transcript (Figure 6A), *hoxb5a* morphants resembled wild-type embryos (Figures 6D and 6E). The enlarged hearts of *hoxb5b* morphants were especially intriguing (Figure 6G), so we assessed the number of cells in each cardiac chamber. Strikingly, *hoxb5b* morphants contain an increased number of atrial cells at 48 hpf and an increased number of cells expressing *amhc* prior to heart tube assembly (Figures 6I, 6J, 6L–6O, 6Q, and 6R; Tables S1 and S2). However, neither ventricular cell number nor *vmhc* expression is affected in *hoxb5b* morphants (Figures 6I–6K, 6M–6P, and 6R; Tables S1 and S2). Interestingly, the increases in atrial cell number were similar to those found in DEAB-treated and RO-treated embryos (Figures 1D and 1E; Figures S2T and S2Y). We therefore wondered whether any APs are found within the forelimb field of *hoxb5b* morphants, as was observed in RA signaling-deficient embryos. Fate mapping of *hoxb5b* morphants revealed that atrial cells do occasionally originate within the forelimb field, although not nearly as frequently as in the fate maps of embryos deficient in RA signaling (Figures 3G–3J). Consistent with this, we did not observe a posterior expansion of *gata4* or *nkx2.5* at the 8 somite stage in *hoxb5b* morphants (Table S6). This suggests that the majority of the excess atrial cells in *hoxb5b* morphants arise from the heart field.

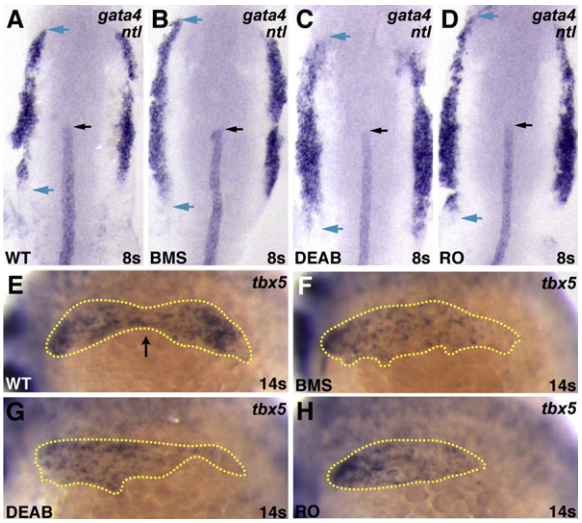

Figure 4. Altered Expression of *gata4* and *tbx5* in Embryos Deficient in RA Signaling

(A–D) Expression at the 8 somite stage of *gata4* and *ntl* in WT, BMS-treated, DEAB-treated, and RO-treated embryos; dorsal views, anterior to the top. When RA signaling is reduced, the total extent of *gata4* expression is longer (blue arrows). This shift in *gata4* expression is most prominent posterior to the notochord tip (black arrow).

(E–H) Expression of *tbx5* in WT, BMS-treated, DEAB-treated, and RO-treated embryos at the 12 somite stage; lateral views, anterior to the left. (E) In WT embryos at this stage, the total extent of *tbx5* expression (yellow outline) is divided into two comparably sized populations; a black arrow indicates the separation point. (F–H) When RA signaling is reduced, the separation between populations is less evident.

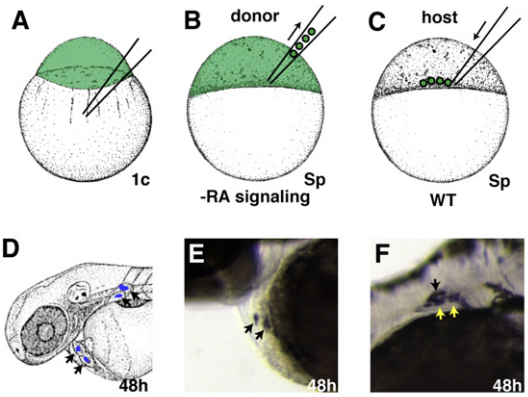

G	DN -heat		DN +heat	
	Freq.	n	Freq.	n
F	30.8%	40	*6.1%	8
A	20.8%	27	19.8%	26
V	24.6%	32	16.0%	21
TT		130		131

H	WT		BMS	
	Freq.	n	Freq.	n
F	20.5%	17	*10.7%	21
A	20.5%	17	17.9%	35
V	24.1%	20	26.0%	51
TT		83		196

Figure 5. Mosaic Analysis Demonstrates a Cell-Autonomous Requirement for RA Signaling during Forelimb Formation

(A–F) Experimental design for mosaic analysis. (A) Donor embryos were injected with fluorescein dextran at the one-cell stage. (B and C) At sphere stage, blastomeres from WT, *Tg(hsp70:dnRARα)*, or BMS-treated donor embryos were transplanted into the margin of a WT host embryo. (D) At 48 hpf, progeny of donor-derived cells (arrows) were detected in the heart and fin by anti-fluorescein immunohistochemistry. (E) Mosaic embryo containing donor-derived cardiomyocytes. (F) Mosaic embryo containing donor-derived cells in pectoral fin. Only LPM-derived fin cartilage cells (yellow arrows), and not fin ectoderm (black arrow) or somite-derived fin muscle (Haines and Currie, 2001; Neyt et al., 2000), were scored as fin.

(G and H) Frequency of heart and fin contributions from heat-shocked *Tg(hsp70:dnRARα)*, non-heat-shocked *Tg(hsp70:dnRARα)*, WT, or BMS-treated donor-derived cells. Percentages reflect the number of mosaic embryos exhibiting donor-derived fin mesenchyme (F), atrial (A), or ventricular (V) cardiomyocytes relative to the total number of transplantation (TT) experiments. Asterisks indicate statistically significant differences from WT ($p < 0.05$).

The distance between *hoxb5b* expression and the heart field (Figures 3A, 3B, 3D, and 3F; Figures S5J–S5L) strongly suggested that *hoxb5b* acts through a nonautonomous mechanism to restrict atrial cell number. We performed two types of mosaic analysis to test this hypothesis. First, we examined whether a *hoxb5b*-deficient environment would affect the contribution of wild-type cells to the atrium. We transplanted cells from wild-type donor embryos into *hoxb5b* morphant or *hoxb5a* morphant host embryos, the latter of which served as controls (Figures 7A–7F). We found a 1.5-fold increase in the frequency with which donor cells contributed to the atrium in *hoxb5b* morphant hosts relative to control *hoxb5a* morphant hosts (Figure 7G), correlating with the 1.5-fold difference in atrial cell number between *hoxb5b* morphants and wild-type embryos. We did not detect a comparable difference in the frequency of donor cells contributing to the ventricle (Figure 7G). These results suggest that *hoxb5b* plays a cell-nonautonomous role in restricting atrial cardiomyocyte formation.

Next, we tested whether ectopic sources of *hoxb5b*, outside of the heart field, can rescue the atrial cardiomyocyte surplus found in *hoxb5b* morphants. In these experiments, we transplanted cells from donor embryos injected with a hyperactive *hoxb5b* (*vp16-hoxb5b*) mRNA into *hoxb5b* morphant hosts; transplants of *hoxb5b* morphant donor cells into *hoxb5b* morphant hosts served as controls (Figures 7H–7K). We then selected chimeras in which donor cells contributed to anterior mesodermal tissues, such as the anterior somites, but did not contribute to the heart, and we assessed cardiac cell number in these embryos. As expected in the control experiments, donor cells from *hoxb5b* morphants had no effect on the *hoxb5b* morphant host phenotype; just as was seen in *hoxb5b* morphants, these chimeras exhibited a 1.5-fold increase in atrial cell number and no significant change in ventricular cell number, relative to wild-type (Figures 7L, 7M, 6O, and 6R). In contrast, donor cells expressing hyperactive *hoxb5b* mRNA caused a statistically significant ($p < 0.05$) reduction of the number of atrial cells in *hoxb5b* morphant hosts (Figures 7L and 7M; Table S1). Thus, we find that expression of *hoxb5b* outside of the heart field can function to restrict atrial cell number. Altogether, we conclude that expression of *hoxb5b*, which is regulated by RA signaling within the forelimb field, plays an essential and cell-nonautonomous role in restricting the production of atrial cardiomyocytes.

DISCUSSION

Synthesizing our data, we propose a model in which interaction between the forelimb field and the heart field acts to restrict the

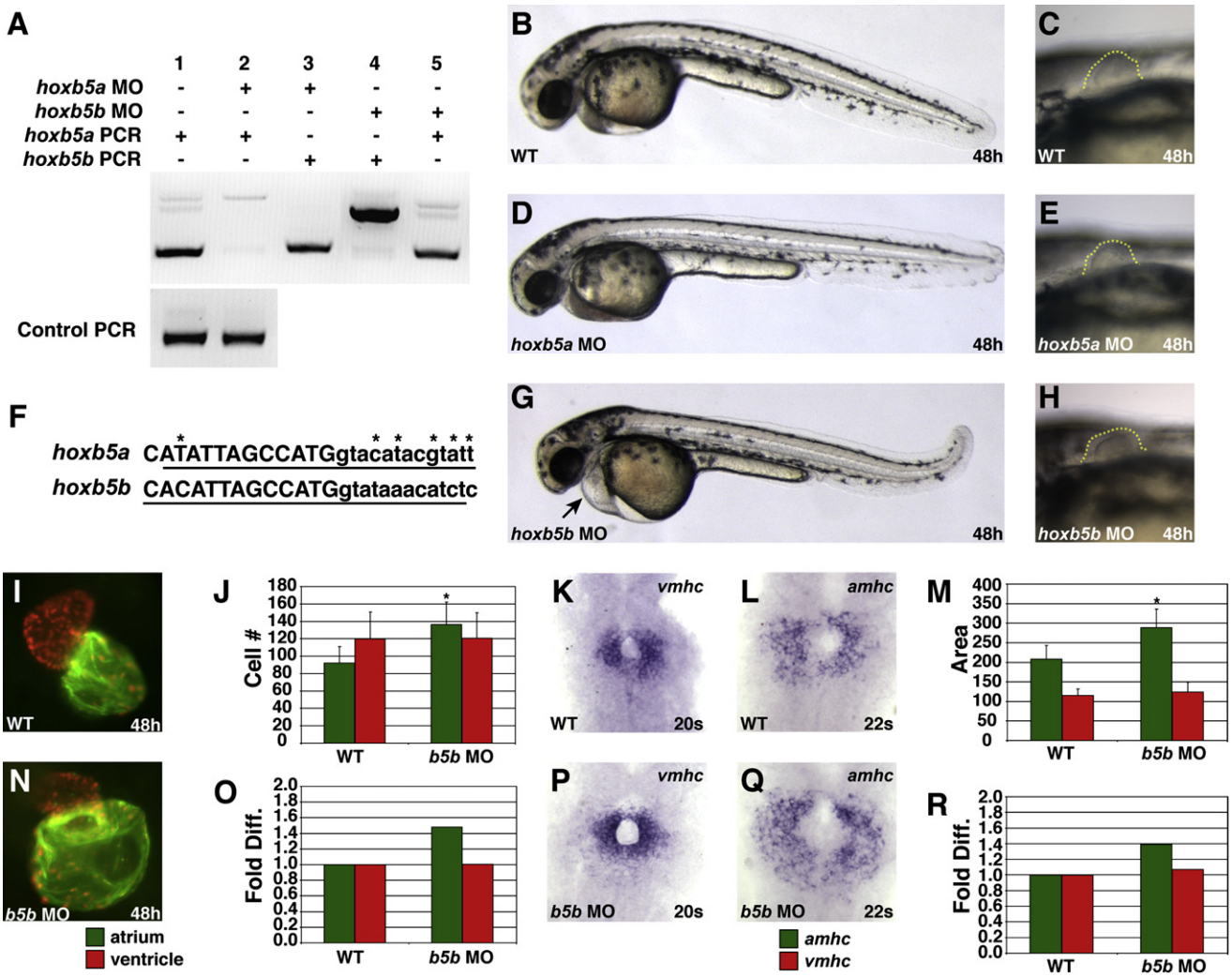

Figure 6. *hoxb5b* Morphants Display an Increased Number of Atrial Cardiomyocytes

(A) MOs targeting the donor site of the single intron in either *hoxb5a* or *hoxb5b* efficiently abrogate splicing of the respective transcript without affecting the other transcript. Larger bands in lanes 2 and 4 represent the retained introns of *hoxb5a* and *hoxb5b*, respectively.

(B–E, G, and H) *hoxb5a* morphants have no evident morphological defects, and *hoxb5b* morphants exhibit enlarged hearts, pericardial edema, and overtly normal pectoral fins. Lateral views, anterior to the left, 48 hpf, with higher magnification of pectoral fin outlined in (E), (G), and (H). (F) Genomic intron-exon structure is completely conserved and nucleotide sequences are highly conserved in the locations that we targeted with anti-*hoxb5b* and anti-*hoxb5a* MOs. Uppercase letters designate first exon sequence, and lowercase letters are intronic sequence. Underline indicates the respective MO target sequences. Asterisks indicate sequence differences.

(I–R) *hoxb5b* morphants display an increased number of atrial cardiomyocytes and a normal number of ventricular cardiomyocytes. Views and graphs are as presented in Figure 1. Error bars represent SD.

number of cardiac progenitor cells. The forelimb and heart fields are juxtaposed during early stages of LPM development, and RA signaling acts cell-autonomously within the forelimb field to induce formation of FPs and expression of RA-responsive genes, including *hoxb5b* (Figure 7N). These effects of RA signaling indirectly result in repression of both AP and VP formation within the heart field, and, in embryos deficient in RA signaling, the expanded AP and VP populations occupy the space created by the loss of the forelimb field (Figure 7O). Hoxb5b plays a key role in the restriction of CP formation; although Hoxb5b is not essential for forelimb formation, it is required to limit atrial cell number through a cell-nonautonomous mechanism (Figure 7P). Thus, we conclude that communication from the forelimb field, mediated at least in part by genes downstream of Hoxb5b, instructs the heart field to limit production of atrial cardiomyocytes, and we speculate that an independent pathway downstream of RA signaling plays a similar role in limiting ventricular cell number.

Our studies offer insight into the mechanisms by which RA signaling both promotes forelimb development and restricts heart size. The direct impact of RA signaling on the forelimb appears relatively straightforward: RA signaling promotes FP formation in the forelimb field. This role is consistent with prior work in zebrafish and mouse suggesting that RA produced by the paraxial

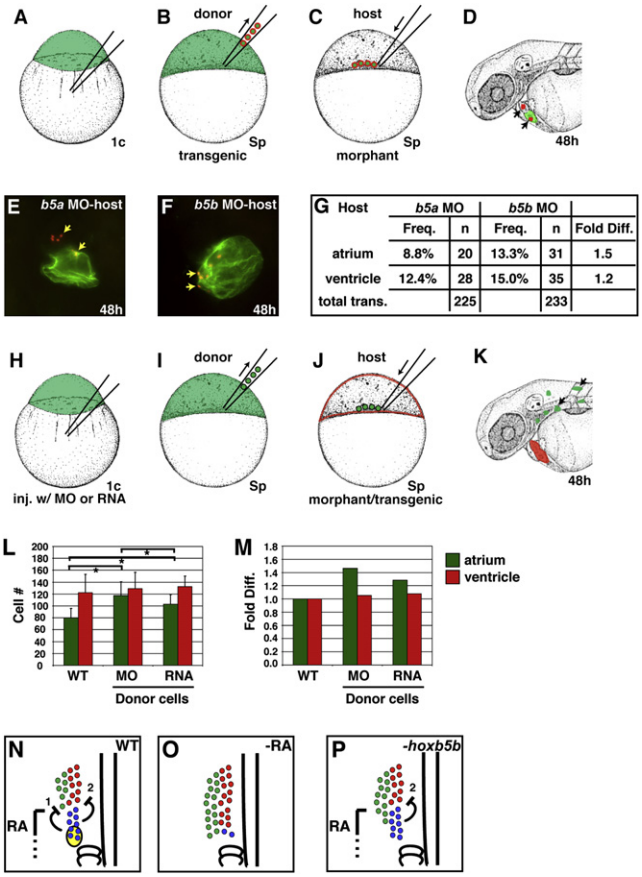

Figure 7. Hoxb5b Acts Nonautonomously to Restrict Atrial Cell Number

(A–D) Experimental design for transplantation of WT donor cells into morphant host embryos. (A) WT donor embryos carrying *Tg(cmlc2:DsRed2-nuc)* were injected with fluorescein dextran at the one-cell stage. (B and C) At sphere stage, donor blastomeres were transplanted into the margin of *hoxb5a* or *hoxb5b* morphant host embryos. (D) At 48 hpf, cardiomyocyte progeny of donor-derived cells (arrows) were detected on the basis of their nuclear DsRed localization. Fixation destroys the fluorescence of the fluorescein dextran lineage tracer, allowing for clean visualization of Amhc (green).

(E) Example of donor cells (arrows) contributing to both the atrium and the ventricle in a *hoxb5a* morphant host.

(F) Example of donor cells (arrows) contributing to the atrium in a *hoxb5b* morphant host.

(G) Frequency of donor cell contributions to each cardiac chamber in *hoxb5a* and *hoxb5b* morphant hosts.

(H–K) Experimental design for transplantation of *hoxb5b* morphant or mRNA-injected donor cells into morphant host embryos. (H) WT donor embryos were injected with *hoxb5b* MO or hyperactive *hoxb5b* mRNA along with fluorescein dextran at the one-cell stage. (I and J) At sphere stage, donor blastomeres were transplanted into the margin of *hoxb5b* morphant host embryos carrying the transgene *Tg(cmlc2:DsRed2-nuc)*. (K) At 48 hpf, we selected host embryos in which donor-derived cells contributed to anterior mesoderm lineages other than the heart and counted the number of cardiomyocytes in each of these hosts.

(L and M) Donor-derived cells expressing hyperactive *hoxb5b* nonautonomously reduce the number of atrial cells in *hoxb5b* morphant embryos. Asterisks represent statistically significant differences between the pair of values indicated by each bar. Error bars represent SD.

(N–P) Model of interactions between the forelimb field and heart field that restrict the number of CPs. (N) RA signaling acts on the forelimb field to promote formation of FPs (blue) and expression of RA-responsive genes, including *hoxb5b* (yellow oval). This indirectly results in production of two hypothesized repressive signals that limit formation of (1) APs (green) and (2) VPs (red). (O) In the absence of RA signaling, the expanded AP and VP populations occupy the space created by the loss of FPs. (P) Without *hoxb5b*, hypothesized to regulate repressive signal 1, FPs are intact and still restrict VP formation, but the AP population is expanded.

mesoderm initiates forelimb development and promotes *tbx5* expression in the forelimb field, although previous studies did not demonstrate the cell-autonomy of this role of RA signaling (Begemann et al., 2001; Capdevila and Izpisua Belmonte, 2001; Gibert et al., 2006; Grandel et al., 2002; Mic et al., 2004; Robert and Lallemand, 2006). It is unclear what happens to aspiring FPs when RA signaling is inhibited. CPs and FPs originate from nearly the same zone of the 40% epiboly embryo (Keegan et al., 2004), and the anterior-posterior organization of CPs and FPs emerges during or shortly after gastrulation as the LPM forms. In RA signaling-deficient embryos, the posterior extension of CPs into the region normally occupied by FPs does not represent a canonical anterior-posterior transformation, since FPs do not seem to be transformed into CPs. Instead, we envision that CPs could come to occupy a more posterior position in the LPM by passively filling the FP void, which may be why we do not see a major posterior displacement of APs in *hoxb5b* morphants. Perhaps the aspiring FPs transform into another, nonmyocardial lineage, although we have not discerned increases in other cell types, including the endocardium (J.S.W. and D.Y., unpublished data), in RA signaling-deficient embryos, consistent with our previous analysis of the endocardial lineage in BMS-treated embryos (Keegan et al., 2005). Alternatively, FPs may simply fail to thrive without early receipt of RA signaling; we have not found evidence of decreased proliferation or cell death within the forelimb field of RA signaling-deficient embryos (Table S7), but a gradual loss of cells would be difficult to detect.

In contrast to the direct role of RA within the forelimb field, the indirect impact of RA signaling on the heart field relies on the effects of RA-responsive genes, like *hoxb5b*, that are expressed in the forelimb field. The pectoral fins appear intact in *hoxb5b* morphants that exhibit a surplus of atrial cells, again emphasizing that the forelimb field is not likely to be the source of extra cardiac cells in this scenario. Additional CPs may form via fate transformation of a yet unidentified lineage or via increased proliferation of CPs. The latter model is particularly appealing to consider for the origin of extra atrial cells, since our 40% epiboly fate maps suggest that RA signaling limits the number of cardiomyocytes produced by individual APs (Figure 1O). We have not been able to detect differences in proliferation within the heart fields of RA signaling-deficient embryos through examination of phospho-histone H3 modification or BrdU incorporation (Table S7; J.S.W. and D.Y., unpublished data), but these negative data cannot rule out a modest or gradual impact on CP cell cycle length. Alternatively, the emergence of additional CPs may reflect utilization of otherwise dormant developmental potential that resides within the heart field.

Our data indicate that RA acts via separable mechanisms to limit the numbers of both ventricular and atrial cardiomyocytes. Several aspects of our conclusions are consistent with previous studies in amniotes. Our observation of a posterior extension of the heart field in zebrafish deficient in RA signaling is reminiscent of the posterior extension of the SHF in mice lacking Raldh2

(Ryckebusch et al., 2008; Sirbu et al., 2008). Likewise, our fate maps at the 8 somite stage (Figures 3F–3I) are comparable to chick fate maps demonstrating that reduced RA signaling causes a posterior expansion of VPs into territory normally containing APs (Hochgreb et al., 2003). In the chick embryo, this expansion is thought to be at the expense of atrial progenitors, although a tradeoff with noncardiac lineages remains a possibility (Hochgreb et al., 2003).

Despite similarities in the roles of RA across species, our data do not support a model in which RA signaling is necessary to partition the heart by promoting formation of atrial cardiomyocytes at the expense of ventricular cardiomyocytes, as suggested by previous analyses of amniotes (Hochgreb et al., 2003; Simoes-Costa et al., 2005; Xavier-Neto et al., 1999, 2001; Yutzey and Kirby, 2002; Yutzey et al., 1994). It is clear from our studies in zebrafish that loss of RA signaling increases atrial cell number. Furthermore, although reduced RA signaling causes increased ventricular cell number in zebrafish, this increase does not occur at the expense of the atrium. It is interesting to note that the excess SHF progenitors in *Raldh2* mutant mice fail to differentiate normally (Ryckebusch et al., 2008). Therefore, we speculate that RA may play similar roles in fish and amniotes at early stages, during restriction of progenitor specification, while also playing different roles during later steps of differentiation and morphogenesis (Chen et al., 1998, 2002; Kastner et al., 1997; Niederreither et al., 1999, 2001). Future studies in amniotes should help to resolve the distinctions between roles of RA at different stages.

The proposed role for RA signaling in partitioning the amniote heart has also led to an evolutionary model that the two-chambered fish heart evolved via subdivision of a single chamber (Simoes-Costa et al., 2005; Xavier-Neto et al., 2001; Yutzey and Kirby, 2002). However, it has also been proposed that the atrium and ventricle arose from independent evolutionary origins (Fishman and Chien, 1997). Our data regarding the independent regulation of atrial and ventricular lineages in zebrafish lend support to the latter model, in which atria and ventricles arose independently, rather than as RA-mediated subdivisions of a single field (Simoes-Costa et al., 2005; Xavier-Neto et al., 2001; Yutzey and Kirby, 2002). Our data therefore suggest that RA signaling does not seem to be an ancestral, conserved mechanism for partitioning the heart field into AP and VP populations.

Our demonstration that *hoxb5b* acts downstream of RA signaling to restrict cardiac cell number suggests that the effects of RA on the heart field are mediated indirectly via genes expressed elsewhere, although this does not exclude the possibility that RA signaling may also have additional roles within the heart field. We favor the interpretation that *hoxb5b* regulates heart field size from its site of expression in the forelimb field, but we cannot rule out that it influences the heart via its expression in the neural tube. However, numerous other *hox* genes, which may function redundantly with *hoxb5b*, are expressed together with *hoxb5b* in the ectoderm (Prince et al., 1998a, 1998b), while we have yet to find another *hox* gene with similar expression in the forelimb field. We suspect that the nonautonomous effect of *hoxb5b* on the heart field involves downstream transcriptional targets that allow the forelimb field to communicate with the adjacent heart field. One possibility is that this communication occurs through the control of a morphogen gradient, as has been shown for Hox control of organ size in *Drosophila* (Crickmore and Mann, 2006, 2007). The specific impact of *hoxb5b* function on atrial, but not ventricular, cell numbers in zebrafish supports a model in which RA signaling limits atrial and ventricular cell numbers through independent downstream pathways. Identification of the relevant targets of Hoxb5b and elucidation of the pathway limiting ventricular cell number will both be important future endeavors.

It is important to consider whether the role of a *Hox* gene in delimiting the heart field may be conserved in amniotes. Although mouse *Hoxb5* mutants display homeotic defects in vertebral patterning and a shift in position of the shoulder girdle, they do not appear to exhibit heart defects (McIntyre et al., 2007; Rancourt et al., 1995). Perhaps subtle cardiac defects are indeed present in *Hoxb5* mutants; addition of extra atrial cells might not be immediately obvious or lethal. Alternatively, other mouse *Hox* genes may be contributing to the role played by zebrafish *hoxb5b*. Multiple Hox genes are expressed in or near the amniote heart field (Ryckebusch et al., 2008; Searcy and Yutzey, 1998), and the mouse *Hoxa3* mutant has been reported to have defects in cardiac development (Chisaka and Capecchi, 1991; Lo and Frasch, 2003). *Hoxa3* mutants display a number of intriguing phenotypes that could be related to alteration of cardiac cell number, including atrial hypertrophy and enlargement of the great veins, as well as other phenotypes such as patent ductus arteriosus, stenosis of the aortic valve, and improperly formed pulmonary valves. Although these defects have been attributed to problems with neural crest formation (Chisaka and Capecchi, 1991; Lo and Frasch, 2003), it is tempting to speculate that Hoxa3 could also influence the heart fields.

Overall, our data provide evidence for an unexpected mechanism of interaction between the forelimb and heart fields during their development. Despite the eventual distance between the heart and the forelimbs, the juxtaposition of their respective organ fields at early stages has a potent effect on the restriction of heart size. Although the precise spatial relationship between the heart and forelimb fields in amniotes is not yet clear, it is likely that they are juxtaposed as they are in zebrafish (Wilson, 1998). The interaction between heart and forelimb fields is particularly germane to the greater than 100 heritable congenital syndromes that feature both heart and forelimb defects (Wilson, 1998). Only a few of these heart-hand syndromes have been linked to their causative genes; one notable example is Holt-Oram syndrome, which is caused by mutation of *Tbx5* (Basson et al., 1997; Li et al., 1997). Since *Tbx5* is expressed in both the heart and forelimb fields, it is thought to autonomously affect both tissues. Our demonstration that genes in the forelimb field can influence the heart field predicts an alternative, nonautonomous mechanism for the etiologies of heart-hand syndromes: initial defects in forelimb development may indirectly impact heart development. Given this interaction, we speculate that there may be reciprocal influences of the heart field on the forelimb field. Altogether, the identification of the restriction of heart field potential by the forelimb field suggests a general mechanism by which communication between adjacent organ fields contributes to the regulation of organ size.

EXPERIMENTAL PROCEDURES

Immunofluorescence and Cell Counting

Tg(cmlc2:DsRed2-nuc)^{f2} embryos (Mably et al., 2003) were fixed at 48 hpf with 1% formaldehyde in PBS. Embryos were stained with the anti-Amhc

monoclonal antibody S46 (Stainier and Fishman, 1992; gift of F. Stockdale), and S46 was detected using a goat anti-mouse IgG1 secondary antibody conjugated to FITC (Southern Biotechnology Associates). To determine the number of cells in each chamber, embryos were gently flattened under a coverslip, and the fluorescent nuclei in each chamber were counted.

In Situ Hybridization

In situ hybridization was performed as described by Oxtoby and Jowett (1993). All probes used were previously described, with the exceptions of *retd* (IMAGE Clone ID - IRAKp961D08178Q2), *hoxb5a* (IMAGE Clone ID - IMAG p998E1515251Q1), and *hoxb5b* (IMAGE Clone ID - IRALp962P2160Q2). Areas of expression of *amhc* and *vmhc* were measured using ImageJ (http://rsb.info.nih.gov/ij/index.html).

BMS189453, DEAB, and Ro41-5253 Treatments

For all three antagonists of RA signaling, we employed doses that cause heart, hindbrain, forelimb, and pharyngeal endoderm phenotypes resembling those caused by genetic reduction of RA signaling in zebrafish *raldh2* mutants (Begemann et al., 2004; Gibert et al., 2006; Keegan et al., 2005; Kopinke et al., 2006; Maves and Kimmel, 2005). For treatment details, see Supplemental Experimental Procedures.

Microarrays

We compared gene expression profiles from wild-type, BMS-treated, DEAB-treated, and RA-treated embryos at tailbud and 8 somite stages using Affymetrix zebrafish GeneChips. For further details, see Supplemental Experimental Procedures.

Fate Mapping

Fate mapping at 40% epiboly was performed as previously described (Keegan et al., 2004, 2005). Fate mapping at the 8 somite stage was performed as previously described (Schoenebeck et al., 2007), with slight modifications. See Supplemental Experimental Procedures for further details.

Morpholino and RNA Injections

The anti-*raldh2* MO was reported previously (Begemann et al., 2001) and was injected with an anti-*p53* MO to reduce toxicity (Robu et al., 2007). To knock down *hoxb5a* or *hoxb5b*, we injected 25 ng of either anti-*hoxb5a* MO (5′-aatacgtatgtaccatggctaatat-3′) or anti-*hoxb5b* MO (5′-agatgtttataccatggctaatgtg-3′).

For ectopic expression of *hoxb5b*, embryos were injected with 30 pg of *vp16-hoxb5b* mRNA. This construct was made by fusing the *vp16* activation domain directly to the N terminus of zebrafish *hoxb5b*. Overexpression of *vp16-hoxb5b* mRNA posteriorizes embryos in a manner similar to that reported for wild-type *hoxb5b* mRNA (Figure S8; Bruce et al., 2001). We consider *vp16-hoxb5b* to be a hyperactive form of *hoxb5b*, since it appears to be more potent than wild-type *hoxb5b*.

Generation of the *Tg(hsp70:dnRARα)* Transgenic Line

We subcloned a human dominant-negative RARα cassette (hRARΔ403; provided by Charles Sagerström; Damm et al., 1993; Roy and Sagerström, 2004) behind the zebrafish *hsp70* promoter (Halloran et al., 2000) and generated a stable line of transgenic animals. For further details, see Supplemental Experimental Procedures.

Mosaic Analysis

To perform mosaic analysis, we used standard techniques to transplant blastomeres at sphere stage (Ho and Kane, 1990). Further details are provided in Supplemental Experimental Procedures.

Phospho-Histone H3 and Apoptotic Cell Labeling

We used the antibody H6409 (Sigma-Aldrich) to detect phospho-histone H3 and the ApopTag kit (Millipore) for TUNEL staining. Stained cells were detected using an alkaline phosphatase-conjugated secondary antibody and NBT/BCIP.

Imaging

Embryos were examined using Zeiss M2Bio and Axioplan microscopes. Photographs were taken using a Zeiss Axiocam. Zeiss AxioVision 3.0.6 software and Adobe Photoshop were used to process images.

SUPPLEMENTAL DATA

Supplemental Data include eight figures, seven tables, Supplemental Experimental Procedures, and Supplemental References and can be found with this article online at http://www.developmentalcell.com/supplemental/S1534-5807(08)00391-2.

ACKNOWLEDGMENTS

We thank A. Schier, A. Lekven, C. Moens, J. Nance, C. Loomis, and members of the Yelon lab for critical input, B. Conrad for assistance with statistical analysis, C. Zusi for providing BMS189453, and K. Niederreither and S. Zaffran for sharing data prior to publication. This work was supported by grants from the National Institutes of Health to D.Y. and K.D.P. and from the American Heart Association to D.Y. J.S.W. received support from NIH F32 HL083591 and K99 HL091126. B.R.K. received support from the NYU Graduate Training Program in Developmental Genetics (NIH T32 HD007520) and the Medical Scientist Training Program of NYU School of Medicine. The authors have no financial conflicts of interest to disclose.

Received: March 19, 2008
Revised: August 28, 2008
Accepted: September 24, 2008
Published: December 8, 2008

REFERENCES

Ahn, D.G., Kourakis, M.J., Rohde, L.A., Silver, L.M., and Ho, R.K. (2002). T-box gene tbx5 is essential for formation of the pectoral limb bud. Nature *417*, 754–758.

Basson, C.T., Bachinsky, D.R., Lin, R.C., Levi, T., Elkins, J.A., Soults, J., Grayzel, D., Kroumpouzou, E., Traill, T.A., Leblanc-Straceski, J., et al. (1997). Mutations in human TBX5 [corrected] cause limb and cardiac malformation in Holt-Oram syndrome. Nat. Genet. *15*, 30–35.

Begemann, G., and Ingham, P.W. (2000). Developmental regulation of Tbx5 in zebrafish embryogenesis. Mech. Dev. *90*, 299–304.

Begemann, G., Schilling, T.F., Rauch, G.J., Geisler, R., and Ingham, P.W. (2001). The zebrafish neckless mutation reveals a requirement for raldh2 in mesodermal signals that pattern the hindbrain. Development *128*, 3081–3094.

Begemann, G., Marx, M., Mebus, K., Meyer, A., and Bastmeyer, M. (2004). Beyond the neckless phenotype: influence of reduced retinoic acid signaling on motor neuron development in the zebrafish hindbrain. Dev. Biol. *271*, 119–129.

Berdougo, E., Coleman, H., Lee, D.H., Stainier, D.Y., and Yelon, D. (2003). Mutation of weak atrium/atrial myosin heavy chain disrupts atrial function and influences ventricular morphogenesis in zebrafish. Development *130*, 6121–6129.

Bruce, A.E., Oates, A.C., Prince, V.E., and Ho, R.K. (2001). Additional hox clusters in the zebrafish: divergent expression patterns belie equivalent activities of duplicate hoxB5 genes. Evol. Dev. *3*, 127–144.

Capdevila, J., and Izpisua Belmonte, J.C. (2001). Patterning mechanisms controlling vertebrate limb development. Annu. Rev. Cell Dev. Biol. *17*, 87–132.

Chen, J., Kubalak, S.W., and Chien, K.R. (1998). Ventricular muscle-restricted targeting of the RXRalpha gene reveals a non-cell-autonomous requirement in cardiac chamber morphogenesis. Development *125*, 1943–1949.

Chen, T.H., Chang, T.C., Kang, J.O., Choudhary, B., Makita, T., Tran, C.M., Burch, J.B., Eid, H., and Sucov, H.M. (2002). Epicardial induction of fetal cardiomyocyte proliferation via a retinoic acid-inducible trophic factor. Dev. Biol. *250*, 198–207.

Chisaka, O., and Capecchi, M.R. (1991). Regionally restricted developmental defects resulting from targeted disruption of the mouse homeobox gene hox-1.5. Nature *350*, 473–479.

Crickmore, M.A., and Mann, R.S. (2006). Hox control of organ size by regulation of morphogen production and mobility. Science *313*, 63–68.

Crickmore, M.A., and Mann, R.S. (2007). Hox control of morphogen mobility and organ development through regulation of glypican expression. Development *134*, 327–334.

Damm, K., Heyman, R.A., Umesono, K., and Evans, R.M. (1993). Functional inhibition of retinoic acid response by dominant negative retinoic acid receptor mutants. Proc. Natl. Acad. Sci. USA *90*, 2989–2993.

Fishman, M.C., and Chien, K.R. (1997). Fashioning the vertebrate heart: earliest embryonic decisions. Development *124*, 2099–2117.

Garrity, D.M., Childs, S., and Fishman, M.C. (2002). The heartstrings mutation in zebrafish causes heart/fin Tbx5 deficiency syndrome. Development *129*, 4635–4645.

Gibert, Y., Gajewski, A., Meyer, A., and Begemann, G. (2006). Induction and prepatterning of the zebrafish pectoral fin bud requires axial retinoic acid signaling. Development *133*, 2649–2659.

Grandel, H., Lun, K., Rauch, G.J., Rhinn, M., Piotrowski, T., Houart, C., Sordino, P., Kuchler, A.M., Schulte-Merker, S., Geisler, R., et al. (2002). Retinoic acid signalling in the zebrafish embryo is necessary during pre-segmentation stages to pattern the anterior-posterior axis of the CNS and to induce a pectoral fin bud. Development *129*, 2851–2865.

Haines, L., and Currie, P.D. (2001). Morphogenesis and evolution of vertebrate appendicular muscle. J. Anat. *199*, 205–209.

Halloran, M.C., Sato-Maeda, M., Warren, J.T., Su, F., Lele, Z., Krone, P.H., Kuwada, J.Y., and Shoji, W. (2000). Laser-induced gene expression in specific cells of transgenic zebrafish. Development *127*, 1953–1960.

Ho, R.K., and Kane, D.A. (1990). Cell-autonomous action of zebrafish spt-1 mutation in specific mesodermal precursors. Nature *348*, 728–730.

Hochgreb, T., Linhares, V.L., Menezes, D.C., Sampaio, A.C., Yan, C.Y., Cardoso, W.V., Rosenthal, N., and Xavier-Neto, J. (2003). A caudorostral wave of RALDH2 conveys anteroposterior information to the cardiac field. Development *130*, 5363–5374.

Huxley, J.S., and deBeer, G.R. (1934). The mosaic style of differentiation (London: Cambridge University Press).

Jacobson, A.G., and Sater, A.K. (1988). Features of embryonic induction. Development *104*, 341–359.

Kastner, P., Messaddeq, N., Mark, M., Wendling, O., Grondona, J.M., Ward, S., Ghyselinck, N., and Chambon, P. (1997). Vitamin A deficiency and mutations of RXRalpha, RXRbeta and RARalpha lead to early differentiation of embryonic ventricular cardiomyocytes. Development *124*, 4749–4758.

Keegan, B.R., Meyer, D., and Yelon, D. (2004). Organization of cardiac chamber progenitors in the zebrafish blastula. Development *131*, 3081–3091.

Keegan, B.R., Feldman, J.L., Begemann, G., Ingham, P.W., and Yelon, D. (2005). Retinoic acid signaling restricts the cardiac progenitor pool. Science *307*, 247–249.

Kopinke, D., Sasine, J., Swift, J., Stephens, W.Z., and Piotrowski, T. (2006). Retinoic acid is required for endodermal pouch morphogenesis and not for pharyngeal endoderm specification. Dev. Dyn. *235*, 2695–2709.

Li, Q.Y., Newbury-Ecob, R.A., Terrett, J.A., Wilson, D.I., Curtis, A.R., Yi, C.H., Gebuhr, T., Bullen, P.J., Robson, S.C., Strachan, T., et al. (1997). Holt-Oram syndrome is caused by mutations in TBX5, a member of the Brachyury (T) gene family. Nat. Genet. *15*, 21–29.

Lo, P.C., and Frasch, M. (2003). Establishing A-P polarity in the embryonic heart tube: a conserved function of Hox genes in Drosophila and vertebrates? Trends Cardiovasc. Med. *13*, 182–187.

Mably, J.D., Mohideen, M.A., Burns, C.G., Chen, J.N., and Fishman, M.C. (2003). heart of glass regulates the concentric growth of the heart in zebrafish. Curr. Biol. *13*, 2138–2147.

Maves, L., and Kimmel, C.B. (2005). Dynamic and sequential patterning of the zebrafish posterior hindbrain by retinoic acid. Dev. Biol. *285*, 593–605.

McIntyre, D.C., Rakshit, S., Yallowitz, A.R., Loken, L., Jeannotte, L., Capecchi, M.R., and Wellik, D.M. (2007). Hox patterning of the vertebrate rib cage. Development *134*, 2981–2989.

Mercader, N., Fischer, S., and Neumann, C.J. (2006). Prdm1 acts downstream of a sequential RA, Wnt and Fgf signaling cascade during zebrafish forelimb induction. Development *133*, 2805–2815.

Mic, F.A., Sirbu, I.O., and Duester, G. (2004). Retinoic acid synthesis controlled by Raldh2 is required early for limb bud initiation and then later as a proximodistal signal during apical ectodermal ridge formation. J. Biol. Chem. *279*, 26698–26706.

Neyt, C., Jagla, K., Thisse, C., Thisse, B., Haines, L., and Currie, P.D. (2000). Evolutionary origins of vertebrate appendicular muscle. Nature *408*, 82–86.

Niederreither, K., Subbarayan, V., Dolle, P., and Chambon, P. (1999). Embryonic retinoic acid synthesis is essential for early mouse post-implantation development. Nat. Genet. *21*, 444–448.

Niederreither, K., Vermot, J., Messaddeq, N., Schuhbaur, B., Chambon, P., and Dolle, P. (2001). Embryonic retinoic acid synthesis is essential for heart morphogenesis in the mouse. Development *128*, 1019–1031.

Oosterveen, T., Niederreither, K., Dolle, P., Chambon, P., Meijlink, F., and Deschamps, J. (2003). Retinoids regulate the anterior expression boundaries of 5′ Hoxb genes in posterior hindbrain. EMBO J. *22*, 262–269.

Oxtoby, E., and Jowett, T. (1993). Cloning of the zebrafish krox-20 gene (krx-20) and its expression during hindbrain development. Nucleic Acids Res. *21*, 1087–1095.

Prince, V.E., Joly, L., Ekker, M., and Ho, R.K. (1998a). Zebrafish hox genes: genomic organization and modified colinear expression patterns in the trunk. Development *125*, 407–420.

Prince, V.E., Moens, C.B., Kimmel, C.B., and Ho, R.K. (1998b). Zebrafish hox genes: expression in the hindbrain region of wild-type and mutants of the segmentation gene, valentino. Development *125*, 393–406.

Raffin, M., Leong, L.M., Rones, M.S., Sparrow, D., Mohun, T., and Mercola, M. (2000). Subdivision of the cardiac Nkx2.5 expression domain into myogenic and nonmyogenic compartments. Dev. Biol. *218*, 326–340.

Rancourt, D.E., Tsuzuki, T., and Capecchi, M.R. (1995). Genetic interaction between hoxb-5 and hoxb-6 is revealed by nonallelic noncomplementation. Genes Dev. *9*, 108–122.

Robert, B., and Lallemand, Y. (2006). Anteroposterior patterning in the limb and digit specification: contribution of mouse genetics. Dev. Dyn. *235*, 2337–2352.

Robu, M.E., Larson, J.D., Nasevicius, A., Beiraghi, S., Brenner, C., Farber, S.A., and Ekker, S.C. (2007). p53 activation by knockdown technologies. PLoS Genet. *3*, e78.

Rones, M.S., McLaughlin, K.A., Raffin, M., and Mercola, M. (2000). Serrate and Notch specify cell fates in the heart field by suppressing cardiomyogenesis. Development *127*, 3865–3876.

Roy, N.M., and Sagerström, C.G. (2004). An early Fgf signal required for gene expression in the zebrafish hindbrain primordium. Brain Res. Dev. Brain Res. *148*, 27–42.

Russo, J.E., Hauguitz, D., and Hilton, J. (1988). Inhibition of mouse cytosolic aldehyde dehydrogenase by 4-(diethylamino)benzaldehyde. Biochem. Pharmacol. *37*, 1639–1642.

Ryckebusch, L., Wang, Z., Bertrand, N., Lin, S.C., Chi, X., Schwartz, R., Zaffran, S., and Niederreither, K. (2008). Retinoic acid deficiency alters second heart field formation. Proc. Natl. Acad. Sci. USA *105*, 2913–2918.

Schoenebeck, J.J., Keegan, B.R., and Yelon, D. (2007). Vessel and blood specification override cardiac potential in anterior mesoderm. Dev. Cell *13*, 254–267.

Schulze, G.E., Clay, R.J., Mezza, L.E., Bregman, C.L., Buroker, R.A., and Frantz, J.D. (2001). BMS-189453, a novel retinoid receptor antagonist, is a potent testicular toxin. Toxicol. Sci. *59*, 297–308.

Searcy, R.D., and Yutzey, K.E. (1998). Analysis of Hox gene expression during early avian heart development. Dev. Dyn. *213*, 82–91.

Sharpe, J., Nonchev, S., Gould, A., Whiting, J., and Krumlauf, R. (1998). Selectivity, sharing and competitive interactions in the regulation of Hoxb genes. EMBO J. *17*, 1788–1798.

Simoes-Costa, M.S., Vasconcelos, M., Sampaio, A.C., Cravo, R.M., Linhares, V.L., Hochgreb, T., Yan, C.Y., Davidson, B., and Xavier-Neto, J. (2005). The evolutionary origin of cardiac chambers. Dev. Biol. *277*, 1–15.

Sirbu, I.O., Zhao, X., and Duester, G. (2008). Retinoic acid controls heart anteroposterior patterning by down-regulating Isl1 through the Fgf8 pathway. Dev. Dyn. *237*, 1627–1635.

Stainier, D.Y., and Fishman, M.C. (1992). Patterning the zebrafish heart tube: acquisition of anteroposterior polarity. Dev. Biol. *153*, 91–101.

Wilson, G.N. (1998). Correlated heart/limb anomalies in Mendelian syndromes provide evidence for a cardiomelic developmental field. Am. J. Med. Genet. *76*, 297–305.

Xavier-Neto, J., Neville, C.M., Shapiro, M.D., Houghton, L., Wang, G.F., Nikovits, W., Jr., Stockdale, F.E., and Rosenthal, N. (1999). A retinoic acid-inducible transgenic marker of sino-atrial development in the mouse heart. Development *126*, 2677–2687.

Xavier-Neto, J., Rosenthal, N., Silva, F.A., Matos, T.G., Hochgreb, T., and Linhares, V.L. (2001). Retinoid signaling and cardiac anteroposterior segmentation. Genesis *31*, 97–104.

Yelon, D., Horne, S.A., and Stainier, D.Y. (1999). Restricted expression of cardiac myosin genes reveals regulated aspects of heart tube assembly in zebrafish. Dev. Biol. *214*, 23–37.

Yutzey, K.E., and Kirby, M.L. (2002). Wherefore heart thou? Embryonic origins of cardiogenic mesoderm. Dev. Dyn. *223*, 307–320.

Yutzey, K.E., Rhee, J.T., and Bader, D. (1994). Expression of the atrial-specific myosin heavy chain AMHC1 and the establishment of anteroposterior polarity in the developing chicken heart. Development *120*, 871–883.